

## Evaluation of correlations for stagnant thermal conductivity of liquid-saturated porous beds of spheres

V. PRASAD, N. KLADIAS,<sup>†</sup> A. BANDYOPADHAYA and Q. TIAN<sup>‡</sup>

Department of Mechanical Engineering, Columbia University, New York, NY 10027, U.S.A.

(Received 6 December 1988 and in final form 3 February 1989)

### INTRODUCTION

A SURVEY of the literature on convective heat transfer experiments in liquid-saturated porous media reveals that the investigators have always encountered problems in predicting accurately the stagnant thermal conductivity of the working medium. Quite often, a mixing rule based on the volume fraction

$$k_m = \varepsilon k_f + (1 - \varepsilon)k_s \quad (1)$$

has been used to estimate the thermal conductivity of the porous bed. However, the measured values of  $k_m$  agree with the predictions made by equation (1) only if  $k_f \simeq k_s$ . This is evident from the experimental data reported by several investigators [1–3]. As has been noted in ref. [1], the larger the difference between the fluid and the solid thermal conductivities, the more the measured values of  $k_m$  vary from the predictions made by equation (1).

Although many investigators have preferred to obtain  $k_m$  by using their own experimental apparatus under stable thermal gradient conditions, it is not always possible to perform the conduction measurements whenever the convection experiments are carried out. As a result, several investigators have employed empirical correlations to predict the stagnant thermal conductivity of the fluid-saturated porous bed. These correlations are generally based on theoretical studies for one or the other conceptual model for the porous matrix, and have sometimes been verified under diverse experimental conditions. The theoretical works on the estimation of  $k_m$  reported thus far can be categorized into two main groups: one assuming unidirectional heat flow and the other considering two-dimensional heat transfer. Deissler and Boegli [4] numerically solved the conduction equation for two-dimensional heat flow by employing the relaxation method for a unit cell of spheres in a cubical array, and showed that the two-dimensional models are more realistic. Their results indicate that the isotherms are highly nonlinear, and the temperature gradients are substantially different in the fluid and solid regions of the cell at low conductivity ratios,  $\lambda$ . Although these authors were partially successful in comparing their predictions with the experimental data for a wide range of  $\lambda$  and  $0.36 \leq \varepsilon \leq 0.50$ , they did not attempt to present a generalized correlation.

Later, Kunii and Smith [5] used the theoretical equations based on a one-dimensional heat conduction model to predict the stagnant thermal conductivities in packed beds of unconsolidated particles as

$$k_m = k_f \left[ \varepsilon + \frac{a_1(1 - \varepsilon)}{a_3 + a_2\lambda} \right] \quad (2a)$$

where  $\lambda$  is the fluid–solid conductivity ratio,  $k_f/k_s$ . The values of  $a_1$ ,  $a_2$  and  $a_3$  are given as

$$a_1 = 1, a_2 = 2/3, a_3 = \phi_2 + 4.63(\varepsilon - 0.26)(\phi_1 - \phi_2) \quad (2b)$$

for  $0.260 \leq \varepsilon \leq 0.476$  where  $\phi_1$  and  $\phi_2$  depend on  $\varepsilon$  and can be obtained from a plot in ref. [5]. Yagi *et al.* [6] verified the appropriateness of equation (2) in predicting the radially effective thermal conductivities by extrapolating the forced convection heat transfer data to a zero velocity.

By considering that a packed bed may consist of a bundle of long cylinders, Krupiczka [7] solved numerically a set of two heat conduction equations in two dimensions with no temperature drop at the solid–fluid interface. He then extended these results to a spherical lattice and proposed a correlation

$$k_m = k_f \lambda^{-n} \quad (3a)$$

where

$$n = 0.280 - 0.757 \log_{10} \varepsilon + 0.057 \log_{10} \lambda \quad (3b)$$

A comparison between Krupiczka's predictions and the experimental data obtained from various sources indicates that the agreement is generally not good for a gas-filled porous matrix [7]. However, equation (3) predicts reasonably well (mostly within 20%) for the liquid-saturated packed beds.

Based on a one-dimensional heat flow model for conduction through a packed bed of spherical particles, Zehner and Schlunder [8] presented a correlation for the stagnant thermal conductivity as

$$k_m = k_f \left\{ 1 - \sqrt{1 - \varepsilon} + \frac{2\sqrt{1 - \varepsilon}}{1 - \lambda B} \left[ \frac{(1 - \lambda)B}{(1 - \lambda B)^2} \ln \left( \frac{1}{\lambda B} \right) - \frac{B + 1}{2} - \frac{B - 1}{1 - \lambda B} \right] \right\} \quad (4a)$$

where

$$B = 1.25 \left( \frac{1 - \varepsilon}{\varepsilon} \right)^{10/9} \quad (4b)$$

Many more correlations have been reported in the literature for a porous matrix of spherical and non-spherical particles (see Wakao and Kguei [9] for the compilation). However, the present discussion will be restricted to the beds of spherical particles only.

Since the above correlations (equations (2)–(4)) have never been verified against experimental data obtained from a carefully conducted experiment in which various combinations of solid and fluid are used to produce the porous media, it is very difficult to choose one or the other correlation for any particular application. The objective of the present experimental study is to fill this gap.

### EXPERIMENTAL APPARATUS AND PROCEDURE

A schematic of the experimental apparatus used for the present experiments is shown in Fig. 1. It consists of a 17.8 cm i.d. plexiglass tube bounded at both ends with two circular

<sup>†</sup> Present address: Webster Research Center, Xerox Corporation, North Tarrytown, NY 10951, U.S.A.

<sup>‡</sup> Visiting Scholar from Shanghai Institute of Electric Power, People's Republic of China.

NOMENCLATURE

$a_1, a_2, a_3$	constants in equation (2)	$T_c$	average temperature of the cold surface [K]
$B$	constant in equation (4)	$T_h$	average temperature of the heated surface [K].
$d$	average diameter of spherical beads [mm]		
$k_f$	thermal conductivity of fluid [W m <sup>-1</sup> K <sup>-1</sup> ]		
$k_m$	stagnant thermal conductivity of fluid-saturated porous matrix [W m <sup>-1</sup> K <sup>-1</sup> ]		
$k_s$	thermal conductivity of solid particles [W m <sup>-1</sup> K <sup>-1</sup> ]		
$n$	exponent in equation (3)		
Greek symbols			
$\epsilon$	porosity		
$\lambda$	conductivity ratio, $k_f/k_s$		
$\phi_1, \phi_2$	functions of $\lambda$ (equation (2)).		

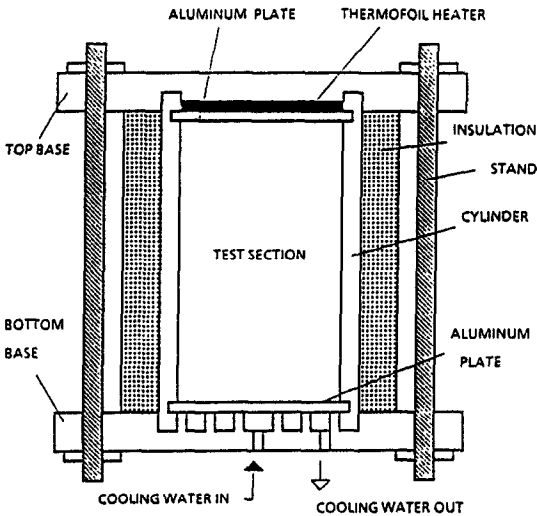


FIG. 1. A schematic of the experimental apparatus.

aluminum plates. On the upper side of the top plate, a circular thermofoil heater of about 15  $\Omega$  is cemented to provide the heat input to the system. The aluminum plate with the heater on the back is then placed in a recess made in a 25.4 mm thick plexiglass plate of 229  $\times$  229 mm dimension. The bottom aluminum plate is also attached to a 25.4 mm thick plexiglass sheet of the same dimension but with circular channels slotted into it for cooling water flow. A constant temperature circulator is then used to supply water at room temperature to obtain an isothermal cold surface. The heater end of the test apparatus is permanently fixed and sealed while the other end can be opened to change the working medium in the conduction cell.

Seven thermocouples are implanted at different radial locations in the heated aluminum plate to measure the temperature variation if any, on the hot surface whereas the cold

surface temperature is monitored by five thermocouples. Several thermocouples are also mounted on both sides of the plexiglass plate on the heater end to estimate the conduction loss. A thick insulation is applied to the test apparatus in order to reduce the heat loss. No efforts are thus made to estimate the loss through the side wall. An almost negligible temperature variation on the heated surface in spite of a uniform heat flux applied there assures that the side effects are reasonably small. The temperature variations on the heated and cooled surfaces were well within 2% of the temperature difference across the conduction cell,  $(T_h - T_c)$ .

Before the porous media experiments were performed, the thermal conductivities of water and ethylene glycol were measured at several temperatures to ascertain the reliability of the system. In general, the measured values of  $k_f$  were within 5% of the tabulated values for these two fluids.

The porous media experiments were performed for various combinations of solid beads and saturating liquids (Table 1). For each of these sets, 3–5 readings were taken at the temperature difference,  $(T_h - T_c)$ , varying between 10 and 50°C while the cold wall was always maintained at room temperature. One such set of experimental runs is reported in Table 2. On the other hand, only an average value of  $k_m$  is reported in Table 1, and the variation with respect to temperature has been neglected.

RESULTS AND DISCUSSION

Table 1 presents the measured stagnant thermal conductivity for various combinations of solid and fluid together with the predictions made by equations (1)–(4). As is evident from the glass–water data, equation (1) can predict reasonable values of  $k_m$  only when  $k_f$  is very close to  $k_s$  ( $\lambda \simeq 1$ ) such that the stagnant thermal conductivity obtained from equation (1) does not vary much from either  $k_f$  or  $k_s$ . On the other hand, as the conductivity ratio decreases or increases from a value close to unity, the difference between measured and predicted (equation (1)) values of  $k_m$  increases. For example, if equation (1) is used to obtain  $k_m$  for the water–steel medium, it may be 750% higher than the real value.

Table 1. Measured stagnant thermal conductivity for liquid-saturated porous media compared with the predictions made by equations (1)–(4)

Liquid	Solid	$d$	$\epsilon$	$k_s$	$\lambda$	Stagnant thermal conductivity, $k_m$				
						Measured	Equation (1)	Equation (2)	Equation (3)	Equation (4)
water	glass	3	0.396	1.10	0.560	0.837	0.910	0.831	0.858	0.874
	glass	25.40	0.425	1.10	0.562	0.842	0.894	0.810	0.844	0.842
glycol	glass	6	0.349	1.10	0.235	0.559	0.806	0.656	0.609	0.649
	glass	25.40	0.427	1.10	0.235	0.597	0.741	0.555	0.561	0.583
steel	acrylic	15.88	0.416	37.39	0.007	2.584	21.940	2.167	2.372	2.417
	acrylic	12.77	0.402	0.16	1.630	0.221	0.200	0.206	0.195	0.196
water	acrylic	25.40	0.427	0.16	3.937	0.479	0.358	0.371	0.279	0.308

Table 2. Experimental results for ethylene glycol-chrome steel medium ( $d = 15.88$  mm,  $\varepsilon = 0.416$ ) and predictions made by equations (1)–(4)

$(T_h - T_c)$	$\lambda$	Measured	Stagnant thermal conductivity, $k_m$			
			Equation (1)	Equation (2)	Equation (3)	Equation (4)
24.7	0.0070	2.434	21.59	2.153	2.349	2.395
43.1	0.0070	2.456	21.84	2.163	2.365	2.411
54.0	0.0069	2.571	22.06	1.172	2.379	2.424
58.9	0.0069	2.875	22.29	2.181	2.393	2.437

Table 3. Stagnant thermal conductivity of porous media measured by ref. [3] in a horizontal cavity heated from below (Rayleigh number lower than the critical value required for the onset of convection)

Liquid	Solid	$d$	$\varepsilon$	Stagnant thermal conductivity, $k_m$			
				Measured	Equation (2)	Equation (3)	Equation (4)
water	glass	3	0.375	0.831	0.834	0.831	0.835
	steel	6.35	0.388	4.653	4.676	4.493	4.763
glycol	glass	3	0.400	0.581	0.579	0.542	0.573
	glass	6	0.440	0.524	0.536	0.520	0.544

Table 4. Stagnant thermal conductivity measured by Combarous [10] in a horizontal cavity heated from below, compared with predictions

Liquid	Solid	$d$	$\varepsilon$	$\lambda$	Stagnant thermal conductivity, $k_m$			
					Measured	Equation (2)	Equation (3)	Equation (4)
water	glass	1.7	0.385	0.512	0.87	0.88	0.91	0.93
	glass	4.0	0.371	0.512	0.85	0.89	0.92	0.94
	glass	3.0	0.381	0.512	0.90	0.88	0.91	0.94
oil	glass	0.9	0.359	0.124	0.47	0.53	0.49	0.53
	glass	2.0	0.351	0.124	0.47	0.55	0.49	0.54
water	lead	4.0	0.370	56.94	4.78	5.18	4.81	5.07
water	quartz	1.9	0.350	12.90	2.75	2.96	2.61	2.86
	quartz	2.25	0.335	12.90	2.88	3.15	2.71	2.96
water	quartz	2.25	0.324	12.90	2.85	3.29	2.78	3.04
	polypropylene	4.0	0.360	20.67	0.30	0.24	0.08	0.16

From Tables 1 and 2, it is also clear that all the other three correlations (equations (2)–(4)) are quite capable of predicting reasonable values for  $k_m$  as long as the thermal conductivity of solid is higher than that for the fluid, i.e.  $\lambda < 1$ . When the conductivity ratio is higher than unity, the effectiveness of these equations diminish. Indeed, Table 2 indicates that for glycol-acrylic ( $\lambda = 1.63$ ), the agreement is not as bad as that for the water-acrylic ( $\lambda = 3.94$ ).

The above agreement between the measured values of  $k_m$  and predictions made by equations (2)–(4) is also supported by the experimental data obtained in refs. [3, 10] (Tables 3 and 4). It should be noted that these values of  $k_m$  were obtained in refs. [3, 10] while conducting free convection experiments in a horizontal cavity heated from below (Rayleigh number lower than the critical value required for the onset of convection).

A close look at Tables 1–4 further indicates that equations (3) and (4) generally predict better values of  $k_m$  than equation (2). One of the difficulties associated with equation (2) is that one has to read the charts given in ref. [5]. On the other hand, equations (3) and (4) are easier to use, and the only information required by these correlations are the thermal conductivities of solid and fluid, and the porosity. Equation (3), however, may be more favorable than equation (4) primarily because this correlation is based on the two-dimensional theoretical model and is more convenient to use. Also, we do not recommend the use of any of these correlations for a high conductivity ratio porous medium,

such as water-acrylic ( $\lambda \approx 3.94$ ) and water-polypropylene ( $\lambda \approx 20$ ) in the present case. Further theoretical and experimental studies are thus needed to obtain correlations which can predict accurately the stagnant thermal conductivity for high values of  $\lambda$ .

## CONCLUSION

The stagnant thermal conductivities measured by the present investigators [3, 10], agree reasonably well with the predictions made by the correlations of Kunii and Smith [5], Krupiczka [7], and Zehner and Schlunder [8] as long as the conductivity ratio is not higher than unity. On the other hand, a mixing rule based on the volume fraction (equation (1)) cannot be used to predict  $k_m$  unless  $\lambda \approx 1$ . Since Krupiczka's correlation (equation (3)) is based on the two-dimensional heat transfer model and predicts more accurate values of  $k_m$  than equation (2), it may be a better choice. None of these correlations are, however, suitable for applications when the thermal conductivity of fluid is much higher than that of the solid ( $\lambda > 1$ ).

**Acknowledgements**—This work has been supported in part by the National Science Foundation (Grant No. CBT-85-04100). The last author (Q.T.) appreciates her support from China Government.

## REFERENCES

1. V. Prasad, Natural convection in porous media—an experimental and numerical study for vertical annular and rectangular enclosures, Doctoral dissertation, University of Delaware (1983).
2. T. Jonsson and I. Catton, Effect of Prandtl number on Benard convection in porous media, *J. Heat Transfer* **109**, 371 (1987).
3. N. Kladias, NonDarcy free convection in horizontal porous layers, Doctoral dissertation, Columbia University (1988).
4. R. G. Deissler and J. S. Boegli, An investigation of effective thermal conductivities of powders in various gases, *ASME Trans.* **80**, 1417 (1958).
5. D. Kunii and J. M. Smith, Heat transfer characteristics of porous rocks, *A.I.Ch.E. JI* **49**, 71 (1960).
6. S. Yagi, D. Kunii and N. Wakao, Radially effective thermal conductivities in packed beds, *Int. Dev. Heat Transfer, ASME* **742** (1961).
7. R. Krupiczka, Analysis of thermal conductivity in granular materials (in Polish), *Chemia Stosowana* **2B**, 183 (1966); English Trans. in *Int. Chem. Engng* **7**, 122 (1958).
8. P. Zehner and E. U. Schlunder, Thermal conductivity of granular materials at moderate temperatures (in German), *Chemie-Ingr-Tech.* **42**, 933 (1970).
9. N. Wakao and S. Kguei, *Heat and Mass Transfer in Packed Beds*, Gordon & Breach, New York (1982).
10. M. Combarous, Convection naturelle et convection mixte en milieu poreux, Doctoral dissertation, University of Paris (1970).

*Int. J. Heat Mass Transfer.* Vol. 32, No. 9, pp. 1796–1798, 1989  
Printed in Great Britain

0017-9310/89 \$3.00+0.00  
© 1989 Pergamon Press plc

## Heat and mass transfer to a turbulent falling film—II

A. FAGHRI

Department of Mechanical Systems Engineering, Wright State University, Dayton, OH 45435, U.S.A.

and

R. A. SEBAN

Department of Mechanical Engineering, University of California, Berkeley, CA 94720, U.S.A.

(Received 21 October 1988 and in final form 7 February 1989)

## INTRODUCTION

THIS is a continuation of a previous note [1] on the heat and mass transfer for the turbulent film flow of a binary solution down a wall, with the free surface in contact with the vapor phase of the solvent. In the previous note, the assumption that the transfer coefficients at the surface and at the wall are invariant in the direction of the film flow enabled an algebraic solution for the distributions of the mean concentration and mean temperature for the cases of a constant wall temperature or a constant heat flux at the wall. These results were compared with the numerical solution by Grossman and Heath [2], using for the algebraic solution the asymptotic values of the transfer coefficients for long flow lengths given by these authors [3] to partially correct errors in the coefficients that were given in ref. [2]. The algebraic solution agreed with the numerical solution for the Reynolds number of  $10^4$ , but did not do so for the higher Reynolds number of  $10^5$ , for which the numerical results were presented in ref. [2]. The need for additional results caused a resumption of a numerical solution like that of ref. [4] for heat transfer alone, which had failed when used for the combined heat and mass transfer of the present problem. Changes in longitudinal and lateral incrementing, and the reformulation of the interface boundary condition did not improve the energy and mass balances made, for each longitudinal increment, to test the calculation. Resolution was finally achieved by using double precision; the source of the arithmetic difficulty was not found and the disadvantage of the double precision requirement was accepted for the limited number of results that were obtained.

## RESULTS

The turbulence model was that of Van Driest, modified by the Mills and Chung eddy diffusivity specifications for the region of the interface; this is Model 1 of ref. [4] except that

the Habib and Na diffusivity modification was used as in Model 3 of that reference. Model 3 should have been used entirely but the results of the modified model are acceptable for the comparison of the algebraic and numerical results. The numerical calculations were made for the condition of a constant wall temperature equal to the initial solution temperature, a Lewis number of 200 and an interface flux ratio parameter,  $\lambda$ , equal to 0.01. The Reynolds numbers were 5000,  $10^4$  and  $10^5$  while the Prandtl numbers were 1 and 10. The interface diffusivity model requires other parameters, and these were specified for water at a temperature of 25°C. For a Reynolds number of  $10^4$ , this gives the same diffusivity distribution as does the model of ref. [2], that model only being applicable for water at a temperature like this, as noted in ref. [1]. The inconsistency of this with the Prandtl number chosen for the calculations makes the results illustrative only; for any actual situation the parameters must be consistent with the particular operating condition.

Table 1 gives the values of the mean concentration,  $\bar{\gamma}$ , the mean temperature,  $\bar{\theta}$ , and the interface temperature,  $\theta_1$ , as obtained from the algebraic solution given in ref. [1] and also those obtained from the numerical calculation, which are subscripted with  $N$ . Table 2 contains the asymptotic values of the Nusselt number,  $Nu_1$ , the Sherwood number,  $Sh_1$ , for the interface and the Nusselt number,  $Nu_0$ , for the wall as given by the numerical results. Associated with each of these is the distance,  $\xi_1$ , at which the interface numbers have decreased to 1.05 times their asymptotic values, and at which the wall Nusselt number has increased to 0.95 times its asymptotic value. Table 2 also contains the distance,  $\xi_2$ , at which the mean concentration attains the value of 0.90. Since  $x/\Delta = 0.25Re\xi$ , the film lengths,  $x$ , are obtainable when the film thickness is specified. As an example, the table contains the values of the film length,  $x_2$ , for water at 25°C flowing down a vertical wall. These are very large and they indicate that concentrations like  $\bar{\gamma} = 0.90$  usually cannot be practically obtained with turbulent flow.